Research on Engineering Structures & Materials
www.jresm.org
Research Group

Research Article

Investigation on floor response spectra of a three-story building exposed to near- and far-field earthquakes

Vyshnavi Pesaralanka[a], Kameswara Rao Burugapalli[b], Surya Prakash Challagulla[c]

Department of Civil Engineering, Koneru Lakshmaiah Education Foundation, Vaddeswaram, Guntur, India

Article Info

Article history:

Received 07 Dec 2023
Accepted 18 Mar 2024

Keywords:

Non-structural component;
Floor response spectrum;
Peak component acceleration;
Near-field earthquakes;
Far-field earthquakes

Abstract

Historical earthquakes highlighted structural collapses and non-structural component (NSC) failures. This study aims to analyze NSC behavior during near and far-field earthquakes in a three-story building by studying elastic and inelastic acceleration responses. The investigation delves into floor response spectra and analyzes how NSCs affect floor acceleration responses, aiming to understand the performance of these components. The findings from the analysis indicated that the Floor Response Spectra (FRS) consistently align peaks with elastic and inelastic modal periods. Inelastic FRS notably show reduced floor spectral accelerations compared to elastic FRS. Near-field earthquakes induce 25-30% higher floor acceleration demands in NSCs compared to far-field earthquakes. Peak Component Acceleration (PCA) values differ significantly between near and far field earthquakes, with near-field ones exhibiting notably higher values across all floors. Higher damping ratios in NSCs lead to decreased peaks in the Component Dynamic Amplification Factor (CDAF) spectrum. The inelastic model notably reduces peak values of CDAF by approximately 49.53% to 69.3% for near-field and 51.81% to 64.47% for far-field earthquakes compared to the elastic model. In summary, the examination of peak floor responses against the formulation based on building codes highlights variations, with instances where the formulation either underestimates or overestimates the peak response demands.

1. Introduction

Buildings are attached with non-structural components (NSCs), which are not designed to withstand structural loads (1), have a vital role in ensuring earthquake resilience. The damage to NSCs can lead to substantial economic losses, both directly and indirectly, often surpassing the costs associated with the primary structural members. The damage to non-structural components (NSCs), which encompass crucial and valuable equipment, can greatly interrupt the operations of diverse structures, especially vital facilities like airports, hospitals, and sites of historical or cultural significance [2-3]. These results emphasize the critical necessity of assessing the seismic behavior of components alongside structural elements. Current standards and recommendations largely rely on practical approaches gleaned from previous encounters and engineering knowledge [4]. Hence, it is vital to design NSCs to endure seismic forces, guaranteeing their safety and the uninterrupted operation of buildings post-earthquake. This entails establishing the Floor Response Spectrum (FRS) at the juncture where the non-structural component connects with the main structure.

NSCs can be categorized into different types based on their failure [5]. While there are now precise methods available for accurately estimating seismic demand on both types of non-

*Corresponding author: chsuryaprakash@kluniversity.in
[a]orcid.org/0000-0003-1284-3139; [b]orcid.org/ 0000-0002-6161-2575; [c]orcid.org/0000-0003-0125-1488;
DOI: http://dx.doi.org/10.17515/resm2024.115ea1207rs

structural components, simpler procedures are sometimes necessary in design scenarios [6]. National and international codes offer several straightforward formulas for calculating seismic demand on NSCs. Many seismic codes used in earthquake-prone areas aim to predict the maximum acceleration and thus the maximum inertial force caused by seismic shaking on NSCs. Therefore, this study focuses solely on acceleration-sensitive non-structural components. Examples of acceleration-sensitive non-structural components include suspended building utility systems like pipe systems and cable trays, as well as anchored or free-standing building utility systems or contents.

The floor response spectrum (FRS) method is an analytical approach that operates by separating various considerations [7–13]. Initially, the primary structure undergoes dynamic analysis independently, without factoring in the secondary system's influence. The acceleration response record from the particular floor where NSCs are affixed is employed as data for modeling the NSC and forming the floor response spectrum. As a result, the maximum force required for NSC design can be determined from the resulting FRS. Studies on the seismic performance of elements exposed to ground motion have demonstrated that the amplification of responses in the primary structure increases the likelihood of NSC damage [14]. Investigations into methods for generating FRS were initiated in the 1970s. Traditionally, various approaches treated the NSC and its supporting structure as single degree of freedom (SDOF) systems. Yasui et al. [15] introduced a method for creating smooth design floor response spectra using either the design spectra or ground response spectra as a reference point. They also developed and verified an innovative method for directly ascertaining floor acceleration spectra [16]. Wei Jiang et al. [17] established floor response spectra to assess the seismic demands on nuclear facilities, finding that FRS generated from time history analysis exhibited significant variations, especially in specific tuning scenarios. The investigation of floor response spectra for multi-story structures has been a subject of study [18–22]. Furthermore, the impact of stiffness irregularities on the FRS was examined [23], with the research revealing heightened acceleration amplification at the soft story level. While the relevant literature has documented a variety of FRS generation methods [17,21,24,25]none of them are capable of effectively assessing how the seismic performance of non-structural components is impacted under near and far-field earthquakes.

Prior research has mostly focused on how both structural and non-structural components respond seismically to typical ground motions. However, limited research has specifically addressed the seismic behavior of primary structures subjected to near- and far-field ground motions [26–31]. These investigations have revealed distinct behaviors of buildings under near field versus far field earthquakes. Consequently, there exists a crucial gap in understanding the seismic performance of non-structural components under both near and far-field earthquake conditions. As a result, there is a critical need to explore the seismic performance of non-structural components under both near and far field earthquake excitations. Therefore, this study aims to assess the impact of near and far field earthquake events on floor spectral accelerations. In the process of generating floor response spectra (FRS), the component dynamic amplification factors are particularly important, as they represent the extent to which NSCs are amplified. Consequently, these parameters and spectral data are examined within the context of a specific building model exposed to seismic forces. Subsequently, a comparative analysis is conducted to assess the disparities between the obtained amplification factors and those derived from code-based calculations.

The paper is organized as follows: Section 2 provides a concise overview of the structural model. Section 3 discusses the selection and scaling of ground motions and provides specific details pertinent to this research. In Section 4, the research findings are presented, with a focus on three key response parameters: floor response spectra, peak component

acceleration, and component dynamic amplification factors. The paper concludes in Section 5 with succinct summarizing remarks.

2. Structural Model

A 3-storey (Ground+2) reinforced concrete (RC), 3D moment-resisting bare frame building as shown in Fig. 1 has been considered in this analysis. Each floor height is assumed as 3 m. The building under consideration is a special moment-resisting frame (SMRF) with a consistent 4-meter bay width across all floors. The reinforced concrete (RC) is modelled with an M30 grade concrete, and the reinforcing steel is HYSD 500. Additionally, as per IS 875-Part 2 [32] guidelines, floor finish load and live load are considered to be 1.5 kN/m^2 and 3 kN/m^2, respectively. The initial sizes of columns and beams have been selected in compliance with IS 13920:2016 [33]. In this design, column dimensions are uniform at 350 mm × 350 mm, and beams are consistently sized at 300 mm × 300 mm for all frames. Additionally, the reinforced concrete (RC) slabs is standardized at 150 mm thickness. The structural model underwent analysis and design considerations for both gravity loads and earthquake forces, specifically in accordance with seismic Zone V conditions. This zone, characterized by a zone factor of 0.36, is associated with a hard soil profile. The design details are shown in Fig 2.

Fig. 1. Three-story building model

To evaluate the performance of the model, the elastic and inelastic responses of the bare frame were examined through time-history analysis, utilizing the finite element software package SeismoStruct (34). In linear modelling, beams and columns are represented as elastic frame elements using their gross moment of inertia. In nonlinear modelling, these elements are portrayed as inelastic plastic hinge force-based elements. Following the ASCE 41-17 [35] standard, the nonlinear characteristics of reinforced concrete (RC) elements are replicated using concentrated plastic hinges positioned at both ends of every member. The plastic hinge length, denoted as L_p, is defined in accordance with Paulay and Priestley [36] as being equal to half of the section depth. The actual structural geometry, incorporating the obtained reinforcement through design, is established to generate the moment-curvature diagram.

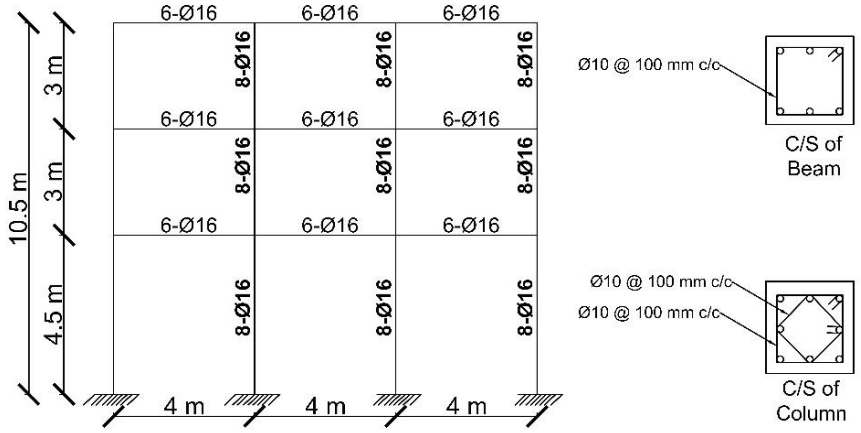

Fig. 2. Reinforcement details of a considered building model

The cracked stiffness of these nonlinear elements is determined following ASCE 41-17 guidelines, which specify the approach for calculating the stiffness of cracked sections for both columns and beams. Mander's model is used to describe the confined concrete's compressive behavior. Steel reinforcement in tension is represented by a bilinear model with isotropic strain hardening behavior. For modelling RC slabs, a rigid diaphragm approach is employed. To simulate the damping effects in the dynamic studies, a Rayleigh damping model has been set up, which accounts for 5% damping divided between the lowest and highest modes to obtain a total of 95% cumulative mass participation in both directions. The analysis considered fixed base conditions, without accounting for soil flexibility. The subsequent section outlines the process employed to choose the ground motion for the current study.

3. Ground Motions

Regarding the assessment of seismic response, realistic responses are generated by utilizing actual ground-motions. Therefore, for the current research, we have incorporated 20 horizontal ground motion excitations, as specified by ASCE 7-16 [37] tailored for hard soil conditions with a shear wave velocity (V_{s30}) greater than 350 m/sec. Additionally, for this study, we have chosen to employ a set of ground-motion records recommended in FEMA P695 [38]. These records will be used to carry out both linear and nonlinear dynamic analyses on the building structures under consideration. Among the set of 20 excitations, 11 of them are categorized as near-field ground motions, while the remaining are classified as far-field ground motions, as detailed in Table 1. According to the classification in FEMA P695, the far-field record set comprises ground motions originating from sites situated at a distance equal to or greater than 10 km from the fault rupture. In contrast, the near-field record set includes ground motions recorded at sites located within a distance of less than 10 km from the fault rupture, as determined by the Joyner-Boore distance (R_{jb}). The ground-motion records under consideration were obtained from sites with rock soil conditions, specifically falling within NEHRP site classes B and C.

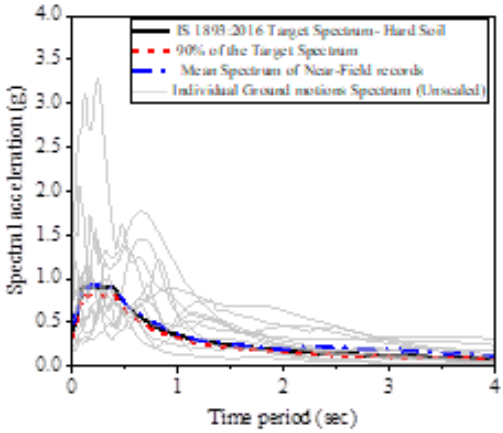

(a)

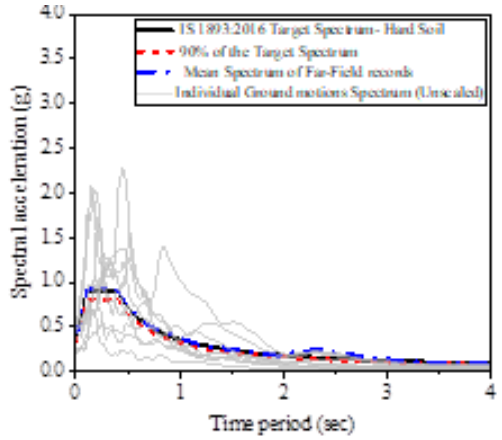

(b)

Fig. 3. Scaled ground motions mean spectra and the target spectrum (a) near-field data, (b) far-field data

These records are associated with moment magnitudes (M_w) ranging from 6.69 to 7.62, with an average magnitude of 7.05. Among the selected records, the closest distances to the fault rupture, calculated as the average Joyner-Boore distance, span from 0 to 26 km, with an average distance of 8.11 km. The epicentral distances (R_{epi}) for this chosen set of ground motions vary between 4.5 and 86 km, with an average distance of 33.4 km. The peak ground acceleration (PGA) values of these selected records range from 0.22 to 1.49 g, and their average PGA is 0.494 g. For more comprehensive information regarding these ground motions, further details can be found in FEMA P695. To achieve compatibility with the target response spectrum, which is the Zone V elastic design spectrum of IS 1893 (Part 1): 2016 [39], the chosen ground motion records were subjected to scaling.

Table 1. Details of near-field and far-field record sets for time-history analysis

S. No	RSN	Earthquake Name	Year	Station Name	M_w	R_{jb} (km)	V_{s30} (m/sec)	PGA (g)	R_{epi} (km)
Near field records									
1	292	Irpinia_ Italy-01	1980	Sturno (STN)	6.9	6.78	382	0.226	30.4
2	802	Loma Prieta	1989	Saratoga - Aloha Ave	6.93	7.58	380.89	0.514	27.2
3	821	Erzican_ Turkey	1992	Erzincan	6.69	0	352.05	0.386	9
4	828	Cape Mendocino	1992	Petrolia	7.01	0	422.17	0.597	4.5
5	879	Landers	1992	Lucerne	7.28	2.19	1369	0.725	44
6	1086	Northridge-01	1994	Sylmar - Olive View Med FF	6.69	1.74	440.54	0.604	16.8
7	1165	Kocaeli_ Turkey	1999	Izmit	7.51	3.62	811	0.165	5.3
8	1529	Chi-Chi_ Taiwan	1999	TCU102	7.62	1.49	714.27	0.303	45.6
9	496	Nahanni_ Canada	1985	Site 2	6.76	0	605.04	0.519	38.04
10	825	Cape Mendocino	1992	Cape Mendocino	7.01	0	567.78	1.49	33.98
11	1004	Northridge-01	1994	LA - Sepulveda VA Hospital	6.69	0	380.06	0.752	44.49
Far-field records									
1	953	Northridge	1994	Beverly Hills-Mulhol	6.7	9.4	356	0.52	13.3
2	1787	Hector Mine	1999	Hector	7.1	10.4	685	0.34	26.5
3	1111	Kobe, Japan	1995	Nishi-Akashi	6.9	7.1	609	0.51	8.7
4	1148	Kocaeli, Turkey	1999	Arcelik	7.5	10.6	523	0.22	53.7
5	900	Landers	1992	Yermo Fire Station	7.3	23.6	354	0.24	86
6	767	Loma Prieta	1989	Gilroy Array #3	6.9	12.2	350	0.56	31.4
7	1633	Manjil, Iran	1990	Abbar	7.4	12.6	724	0.51	40.4
8	1485	Chi-Chi, Taiwan	1999	TCU045	7.6	26	705	0.51	77.5
9	125	Friuli, Italy	1976	Tolmezzo	6.5	15	425	0.35	20.2

The process employed for this purpose involved the utilization of a time-domain spectral matching approach to generate earthquake excitations that align with the desired spectrum. Figure 3 illustrates the target spectrum as per IS 1893:2016, which are linked to 5% damping, along with the mean spectra of ground excitations. It is essential that the mean spectra remain over 90% of the target spectrum for the whole-time range, as per ASCE 7-16 requirements. It is evident (Fig. 3) that the mean spectra comfortably exceed this 90% threshold. Table 2 provides information regarding the modal periods and

cumulative modal mass participation ratios for a three-story building model in both linear and nonlinear analysis ranges.

Table 2. Details of time periods and cumulative mass participation ratios of considered models

Mode	Linear Model			Non-Linear Model		
	T (sec)	UX	UY	T (sec)	UX	UY
Mode 1(Y)	0.743	28.83	64.86	1.71	89.08	3.68
Mode 2(X)	0.742	93.85	93.77	1.70	92.79	92.74
Mode 3(Z)	0.635	93.92	93.92	1.40	92.83	92.82
Mode 4(X)	0.206	97.76	95.51	0.495	99.48	92.82
Mode 5(Y)	0.206	99.36	99.36	0.495	99.48	99.48
Mode 6(Z)	0.178	99.55	99.36	0.415	99.48	99.48
Mode7 (Y)	0.101	99.99	99.80	0.246	99.92	99.55
Mode 8(X)	0.101	99.99	99.99	0.246	99.99	99.99
Mode 9(Z)	0.089	99.99	99.99	0.214	99.99	99.99
Mode 10(X)	0.054	99.99	99.99	0.078	99.99	99.99

Note: T represents Time period, UX and UY are cumulative modal mass participation ratios along X and Y directions.

4. Results and Discussion

The behavior of non-structural components is examined in detail in the following sections. The key response parameters used to characterize the performance of these components include Floor Response Spectra (FRS), Peak Component Acceleration (PCA), and Component Dynamic Amplification Factors (CDAF). It is essential to highlight that this study does not consider component's nonlinearity and is specifically applicable to lightweight components that do not introduce dynamic feedback to the primary structure. In other words, interaction effects between non-structural components and the primary building structure are not considered in this analysis.

4.1 Floor Response Spectrum (FRS)

In the current research, the non-structural components (NSCs) under investigation are elastic single-degree-of-freedom (SDOF) systems. Dynamic interaction effects are disregarded since these NSCs are believed to have a mass much lower than that of the main structure. The methodology employed involves the use of Floor Response Spectra (FRS) as a decoupled approach, allowing for the independent assessment of both the structure and the NSCs in a specified manner. For this purpose, scaled near- and far-field ground motions serve as input data for both linear and non-linear time history analyses. Absolute acceleration responses are individually obtained for all floors and subsequently utilized as input to calculate the corresponding FRS for the NSCs. A 5% damping ratio is used to calculate these FRS, and the average findings for each floor are presented and evaluated. The average spectral acceleration (S_a, measured in g units) of a non-structural component (NSC) connected to a specific floor is graphed in relation to the vibration period (T_s, measured in seconds) for the building model depicted in Figure 4. When the FRS are plotted across an extensive variety of periods, it is predicted that the largest peaks in the spectrum would line up with the fundamental period of the main structure [40]. These observed peaks in the FRS correspond to the modal periods of the building model under consideration.

From Fig.4, it can be observed that the two peaks observed in the elastic and inelastic FRS are recorded close to the structure's elastic and inelastic modal periods (Table 3), respectively. This finding from this study is consistent with the outcomes of the previous research [11–13]. The Floor Response Spectra (FRS) exhibit a consistent trend of increasing magnitude from the first floor at the bottom to the third floor at the top. At first glance, it is evident that the floor spectral accelerations of the inelastic FRS—shown by dotted lines—are significantly lower than its elastic counterpart. The impact of both near-field and far-field excitations on the FRS is evident when observing the magnitude of the peaks. It is observed that, under far-field excitations, the FRS peaks corresponding to modal periods are noticeably lower in magnitude compared to those under near-field excitations.

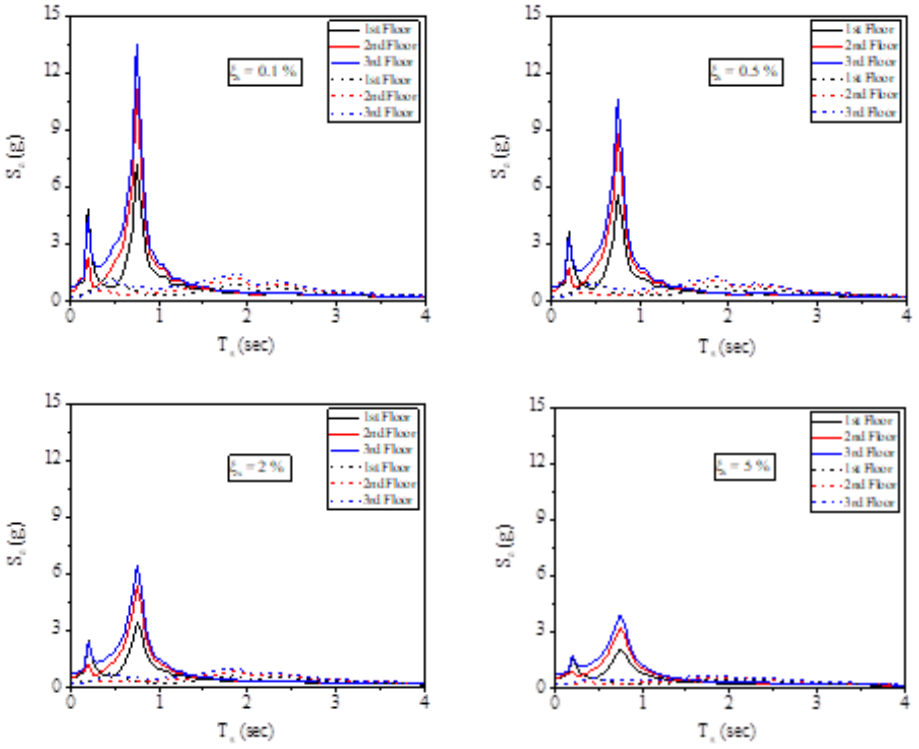

(a)

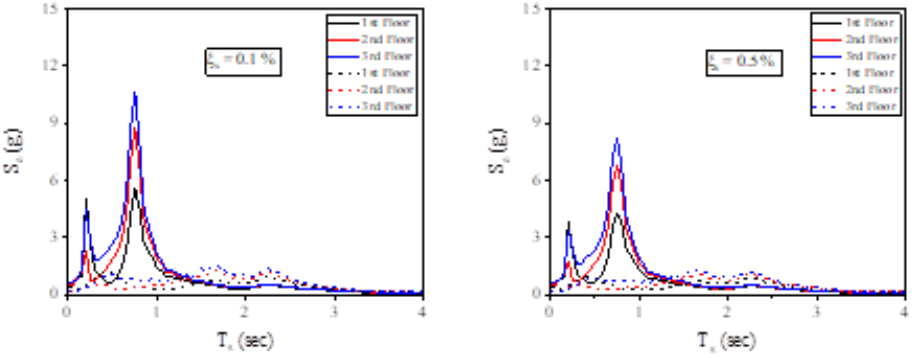

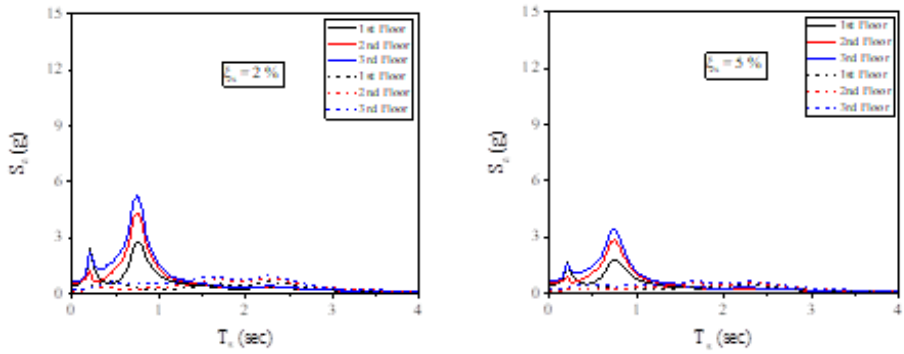

(b)

Fig. 4. Elastic (solid line) and inelastic (dashed line) FRS of 3-storey considered building model for (a) near-field data, (b) far-field data

As an illustration, when considering the higher floor level and an elastic FRS peak associated with the first fundamental period of a building model with a specified damping ratio for the non-structural component (ξ_s = 0.5%), the magnitudes of the floor spectral accelerations are 10.62 g and 8.19 g under near-field and far-field excitations, respectively. Likewise, for the higher floor level and an inelastic FRS peak associated with the first fundamental period of the same building model with the same damping ratio (ξ_s = 0.5%), the magnitudes of the spectral acceleration are 1.28 g and 1.19 g under near-field and far-field excitations, respectively. A significant decrease in floor spectral acceleration is evident when considering far-field excitations. The same pattern is observable for other damping ratios as well. Therefore, we can draw the conclusion that, regardless of the damping ratio of the non-structural component (NSC), near-field excitations lead to higher demands for floor accelerations when compared to far-field excitations. The proximity of the earthquake source plays a critical role in this outcome. Near-field earthquakes, which occur in close proximity to the building, tend to produce ground motions with higher amplitudes and more pronounced high-frequency content. These characteristics can induce higher spectral accelerations and amplification effects in the building's response. In contrast, far-field earthquakes, originating at a greater distance, generally result in ground motions with lower amplitudes and a broader range of frequencies. This typically leads to reduced demands for floor accelerations in the building's response. This conclusion underscores the importance of considering the source-to-site distance and the characteristics of the ground motion when assessing the seismic response of primary structures and non-structural components to withstand earthquakes.

4.2 Peak Component Acceleration

The highest ordinate in the floor response spectrum in the current investigation is referred to as the peak component acceleration (PCA), is subjected to a normalization process with the Peak Ground Acceleration (PGA). Subsequently, the PCA/PGA ratio is graphed in relation to the relative height (z/H, where z is the floor height and H is the total height of the building) of the building model.

Figure 5 highlights a consistent trend across both linear and non-linear analyses, demonstrating a direct relationship between floor elevation and seismic activity. It shows that seismic demands tend to increase as buildings rise, regardless of whether the analysis considers near or far field earthquakes. This suggests a crucial correlation between the floor level and the intensity of seismic effects.

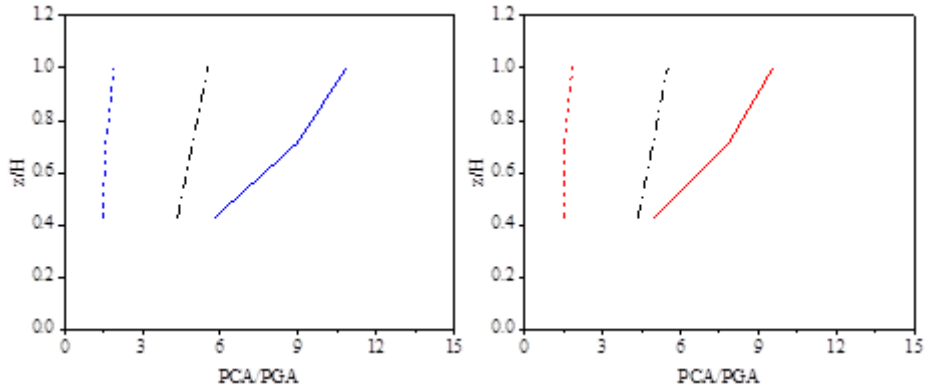

(a) (b)

Fig. 5. Comparison of elastic (solid line) and inelastic (dashed line) FRS of 3-storey considered building model with ASCE 7-16 (dashed-dotted line) formulation for (a) near-field data, (b) far-field data

The comparison between near and far field earthquakes reveals intriguing differences in seismic impact. Near field earthquakes exhibit significantly higher PCA values compared to far field earthquakes. This substantial difference—approximately 15.95% higher for the 1st floor, 14.12% for the 2nd floor, and 13.47% for the 3rd floor—emphasizes a much sharper variation in demands between floors during near field events. This heightened impact likely arises due to the closer proximity of near field earthquakes to the earthquake epicenter. Moreover, the examination of non-linear PCA values unveils additional intricacies. It highlights a nuanced impact, showing a slight decrease in impact on the 1st floor (approximately -1.86%) but a notable increase on the 2nd and 3rd floors (around 4.73% and 3.24% respectively) during near field earthquakes compared to far field earthquakes. These variations underscore the complex relationships in seismic effects across different floors during near field seismic events. Conversely, far field earthquakes showcase lower PCA values across all floors, suggesting a comparatively less pronounced variation in demands between different floor levels.

The PCA/PGA values obtained using the ASCE 7-16 formulation, as defined in Eq. (1), when compared to the results from linear analysis, consistently show lower values across both near and far field earthquake scenarios. This means that the ASCE 7-16 formulation tends to provide estimates of PCA demands that are lower than what the linear analysis suggests.

$$PCA/PGA = a_p\left(1+\frac{z}{H}\right) \tag{1}$$

where, a_p is the component amplification factor. As per the definition of ASCE 7–16, a_p for flexible NSCs with a time period longer than 0.06 sec is 2.5. The value of the a_p is 1 for NSCs whose time period is less than 0.06 sec.

Conversely, when compared to the results derived from non-linear analysis, the PCA values obtained from the ASCE 7-16 formulation tend to be higher across both near and far field earthquake scenarios. This indicates that the ASCE 7-16 formulation tends to overestimate the PCA demands compared to what the non-linear analysis reveals. So, in summary, the ASCE 7-16 formulation generally underestimates the seismic impact when compared to linear analysis and overestimates it when compared to non-linear analysis in both near and far field earthquake situations. As a result, the peak acceleration response of the NSCs cannot be reliably estimated using the present code-based linear formulation. To enhance

accuracy, there's a need to update the formulation to include considerations for both the non-linear behavior of the structure itself and the varied characteristics of ground motions that affect the structure's response during earthquakes.

4.3 Component Dynamic Amplification Factor (CDAF)

The analysis of component acceleration amplification in relation to the floor acceleration is covered in this section. Floor Response Spectra (FRSs) normalized by corresponding Peak Floor Accelerations (PFAs) are analyzed in this process. In Fig. 6, the FRS (elastic and in-elastic) of the building model at the first-floor level normalized by the corresponding PFA is depicted against the T_s. The ratio between FRS and PFA represents the Component Dynamic Amplification Factor (CDAF). The highest point on the CDAF spectrum represents the amplification factor. This study's CDAF for the building model is juxtaposed with the criteria outlined in ASCE 7–16 [37], FEMA P-750 (41) and EuroCode8 . According to ASCE 7–16, flexible NSCs with a time period exceeding 0.06 seconds have a [42]component amplification factor (a_p) of 2.5, while rigid NSCs (with a time period less than 0.06 seconds) have an amplification factor of 1.

Across various analysis types and seismic scenarios, a consistent observation emerges: an increase in the NSC's damping ratio correlates with a decrease in peaks within the CDAF spectrum. Furthermore, these spectra consistently exhibit peaks aligned with the building's modal periods. In near-field earthquakes, for the elastic model and selected NSC damping ratios (0.1%, 0.5%, 2%, and 5%), peak values within the CDAF spectrum associated with the first modal period range between 4.26 and 14.61, contrasting with the inelastic model's range of 2.15 to 4.49. Similarly, under far-field earthquakes, the elastic model's peak values vary from 3.76 to 13, while the inelastic model's range from 2 to 4.63 for the same damping ratios. In both seismic conditions, comparative analysis reveals distinct differences between elastic and inelastic models across various damping ratios. Under near-field earthquakes, the inelastic model showcases percentage decreases in peak values of approximately 49.53%, 56.14%, 64.89%, and 69.3% compared to the elastic model for damping ratios of 5%, 2%, 0.5%, and 0.1%, respectively. Correspondingly, in far-field earthquakes, these reductions amount to about 51.81%, 55.81%, 60.3%, and 64.47% for the same damping ratios. These consistent disparities underscore the significant impact of seismic conditions and damping ratios on the dynamic characteristics and spectral responses, emphasizing the distinct behavior between elastic and inelastic models within the system.

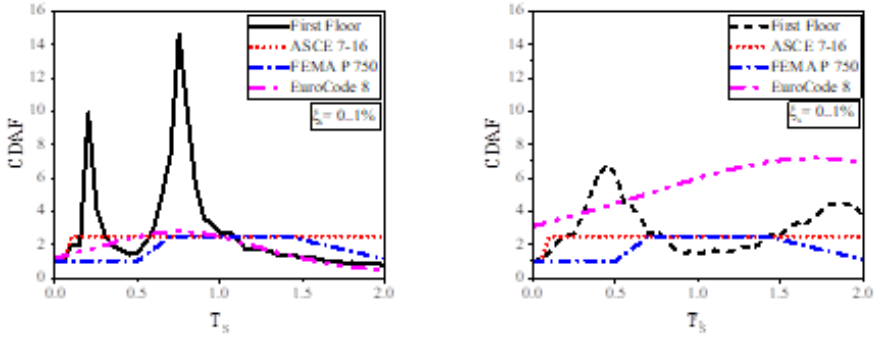

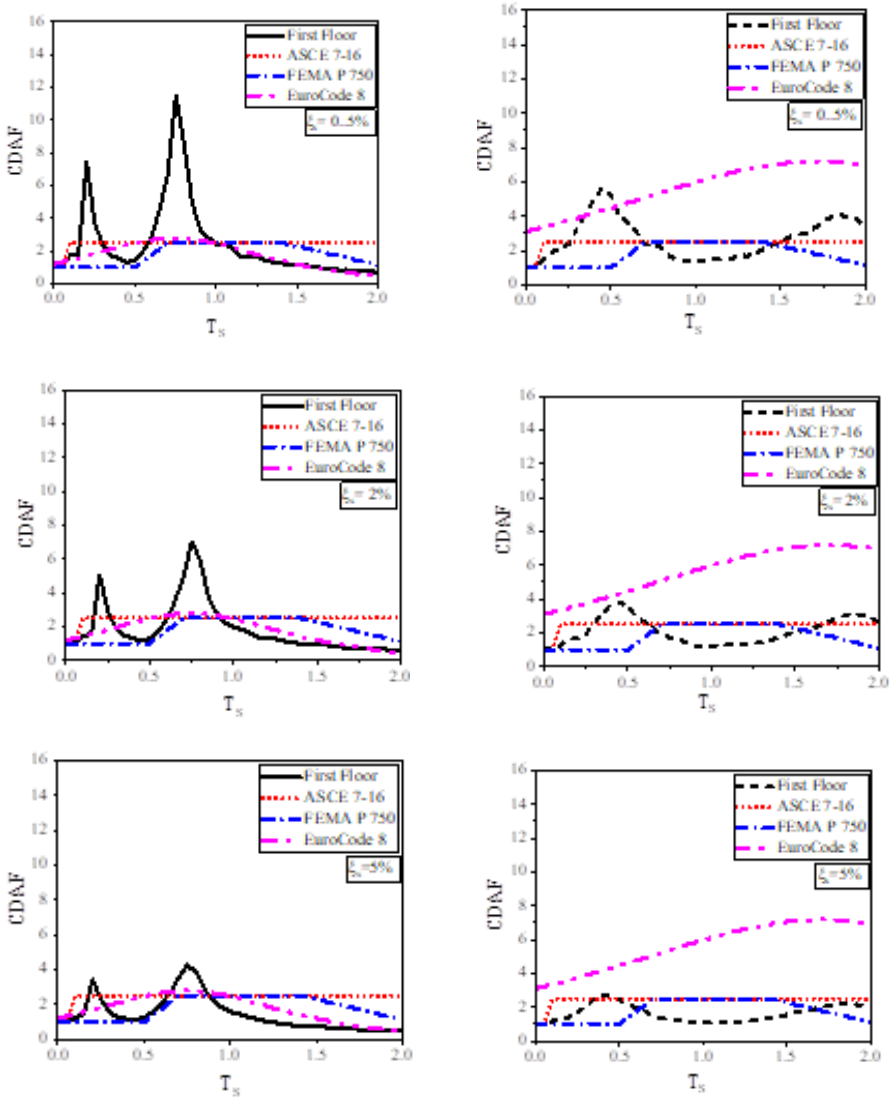
First Floor
ASCE 7-16
FEMA P 750
EuroCode 8
ξs= 0..5%
ξs= 2%
ξs=5%
CDAF
Ts

(a)

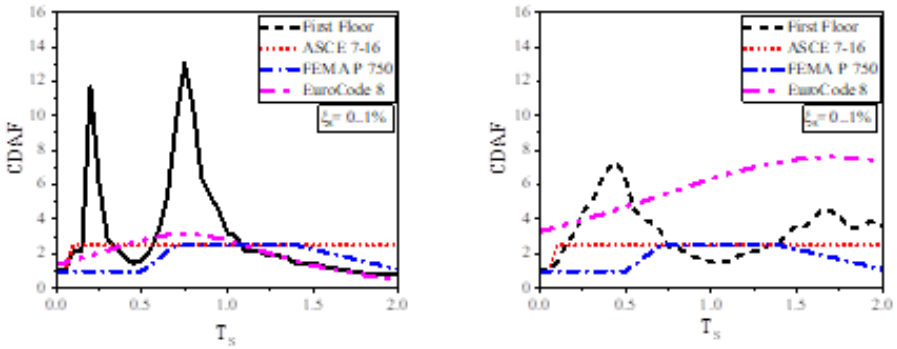
First Floor
ASCE 7-16
FEMA P 750
EuroCode 8
ξs= 0..1%
CDAF
Ts

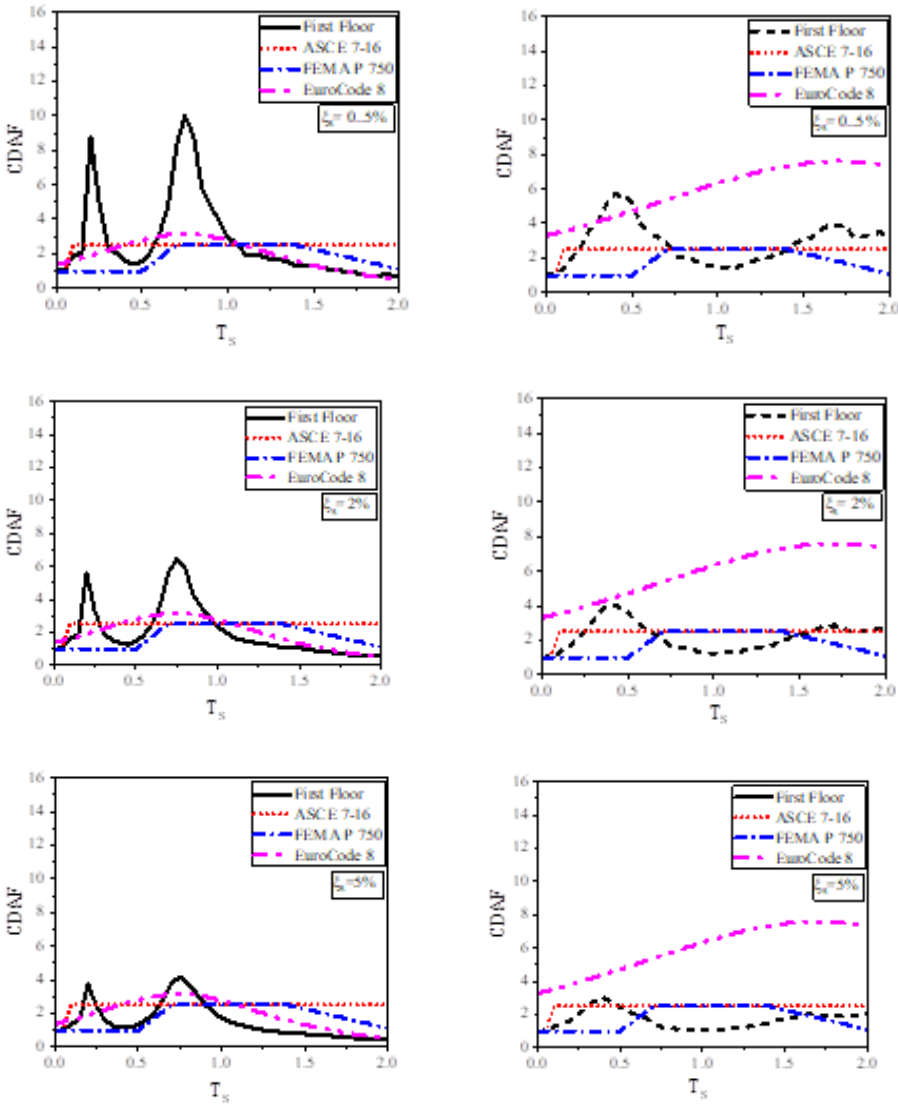

(b)

Fig. 6. Elastic (solid line) and inelastic (dashed line) CDAF spectrum for (a) near-field data, and (b) far-field data

The CDAF spectrum defined by the code-based formulation is plotted and compared against the simulated CDAF spectrum as shown in Fig. 6. In the elastic model, across near and far-field earthquake scenarios, the code-based formulation consistently underestimates the peak CDAF values corresponding to the building's modal periods. Conversely, within the inelastic model, the ASCE formulation consistently overestimates the peak CDAF associated with the first modal period, regardless of the earthquake type. However, both FEMA and Eurocode 8 formulations tend to underestimate the peak CDAF values for damping ratios of 0.1% and 0.5%, whereas for damping ratios of 2% and 5%, they exhibit an overestimation of the CDAF values. Therefore, based on the observed

discrepancies in peak CDAF values attributed to various earthquake types within the elastic and inelastic models, it becomes essential to refine the existing code-based formulation.

5. Conclusions

The current research focuses on analyzing a three-story building model under both near and far-field earthquake conditions. The main aim is to identify and measure the rise in floor acceleration, a crucial factor influencing the design of non-structural components in low-rise buildings for aforementioned earthquakes. The study yields noteworthy findings, summarized as follows:

- In both elastic and inelastic Floor Response Spectra (FRS), observed peaks consistently align closely with the structure's elastic and inelastic modal periods.
- The observed Floor Response Spectra (FRS) consistently depict an ascending trend in magnitude from the building's bottom to top floors. Compared to elastic FRS, the inelastic FRS notably show a considerable decrease in floor spectral accelerations.
- Near-field earthquakes induce 25-30% higher floor acceleration demands in non-structural components compared to far-field earthquakes.
- Near field seismic events exhibit significantly higher Peak Component Acceleration (PCA) values than far field earthquakes. Far field earthquakes display lower PCAs across all floors, suggesting less diverse demands between floor levels.
- Higher damping ratios in the non-structural component led to decreased peaks in the component dynamic amplification factor (CDAF) spectrum. In near-field earthquakes, the inelastic model notably reduces peak values by roughly 49.53% to 69.3% across damping ratios of 0.1% to 5% compared to the elastic model. Similarly, under far-field earthquakes, reductions range from about 51.81% to 64.47% for the same damping ratios in the inelastic model compared to the elastic one.
- The code-based formulations consistently underestimate peak CDAF values in the elastic model, whereas the ASCE formulation consistently overestimates peaks in the inelastic model. FEMA P-750 and Eurocode 8 show varied estimations, either overestimating or underestimating based on specific damping ratios.

The findings of this study are constrained by the specific characteristics of the building model and the selected ground motions. It is important to note that this research focuses solely on the linear response of non-structural components (NSCs) as an initial exploration. To obtain more comprehensive and generalized results, future investigations should incorporate the nonlinear behavior of NSCs. Additionally, there is potential for extending the scope of research to include high-rise structures such as 10, 15, or 20-story buildings with various irregularities. By considering a broader range of building types and structural complexities, future studies can provide deeper insights into the seismic performance of NSCs across different scenarios.

Acknowledgement

The authors acknowledge that this study is supported by Department of Civil Engineering, Koneru Lakshmaiah Education Foundation (KLEF), Vaddeswaram, Guntur, India.

References

[1] Filiatrault A, Perrone D, Merino RJ, Calvi GM. Performance-based seismic design of nonstructural building elements. Journal of Earthquake Engineering. 2021;25(2):237–69.

[2] Shang Q, Wang T, Li J. Seismic fragility of flexible pipeline connections in a base isolated medical building. Earthquake Engineering and Engineering Vibration . 2019;18(4):903–16. https://doi.org/10.1007/s11803-019-0542-5
[3] Di Sarno L, Magliulo G, D'Angela D, Cosenza E. Experimental assessment of the seismic performance of hospital cabinets using shake table testing. Earthq Eng Struct Dyn . 2019 Jan 1;48(1):103–23. https://doi.org/10.1002/eqe.3127
[4] Anajafi H, Medina RA. Evaluation of ASCE 7 equations for designing acceleration-sensitive nonstructural components using data from instrumented buildings. Earthq Eng Struct Dyn . 2018 Apr 10;47(4):1075–94. https://doi.org/10.1002/eqe.3006
[5] Pardalopoulos SI, Pantazopoulou SJ. Seismic response of nonstructural components attached on multistorey buildings. Earthq Eng Struct Dyn. 2015;44(1):139–58.
[6] Perrone D, Andre F. Seismic demand on non-structural elements: Influence of masonry infills on floor response spectra. In: Proceedings 16th European Conference on Earthquake Engineering. 16th European Conference on Earthquake Engineering; 2018.
[7] Suarez LE, Singh MP. Floor response spectra with structure–equipment interaction effects by a mode synthesis approach. Earthq Eng Struct Dyn . 1987 Feb 1;15(2):141–58. https://doi.org/10.1002/eqe.4290150202
[8] Adam C. Dynamics of elastic–plastic shear frames with secondary structures: shake table and numerical studies. Earthq Eng Struct Dyn . 2001 Feb 1;30(2):257–77. https://doi.org/10.1002/1096-9845(200102)30:2<257::AID-EQE7>3.0.CO
[9] Menon A, Magenes G. Definition of Seismic Input for Out-of-Plane Response of Masonry Walls: I. Parametric Study. Journal of Earthquake Engineering . 2011 Jan 5;15(2):165–94. https://doi.org/10.1080/13632460903456981
[10] Challagulla SP, Bhargav NC, Parimi C. Evaluation of damping modification factors for floor response spectra via machine learning model. In: Structures. Elsevier; 2022. p. 679–90.
[11] Challagulla SP, Bhavani BD, Suluguru AK, Jameel M, Vicencio F. Influence of ground motion scaling on floor response spectra. Curr Sci. 2023;124(8):928.
[12] Challagulla SP, Kontoni DPN, Suluguru AK, Hossain I, Ramakrishna U, Jameel M. Assessing the Seismic Demands on Non-Structural Components Attached to Reinforced Concrete Frames. Applied Sciences. 2023;13(3):1817.
[13] Pesaralanka V, Challagulla SP, Vicencio F, Chandra Babu PS, Hossain I, Jameel M, et al. Influence of a Soft Story on the Seismic Response of Non-Structural Components. Sustainability (Switzerland). 2023 Feb 1;15(4).
[14] D'Angela D, Magliulo G, Cosenza E. Seismic damage assessment of unanchored nonstructural components taking into account the building response. Structural Safety . 2021; 93:102126. https://www.sciencedirect.com/science/article/pii/S0167473021000503
[15] Yasui Y, Yoshihara J, Takeda T, Miyamoto A. Direct Generation Method for Floor Response Spectra. In 1993. https://api.semanticscholar.org/CorpusID:199778698
[16] Vukobratović V, Fajfar P. A method for the direct determination of approximate floor response spectra for SDOF inelastic structures. Bulletin of Earthquake Engineering. 2015; 13:1405–24.
[17] Jiang W, Li B, Xie WC, Pandey MD. Generate floor response spectra: Part 1. Direct spectra-to-spectra method. Nuclear Engineering and Design . 2015; 293:525–46. https://www.sciencedirect.com/science/article/pii/S002954931500271X
[18] Calvi P, Sullivan T. Estimating floor spectra in multiple degree of freedom systems. Earthquakes and Structures. 2014 Jul 31; 7:17–38.
[19] Zhai CH, Zheng Z, Li S, Pan X, Xie LL. Seismic response of nonstructural components considering the near-fault pulse-like ground motions. Earthquake and Structures. 2016;10(5):1213–32.

[20] Petrone C, Magliulo G, Manfredi G. Floor response spectra in RC frame structures designed according to Eurocode 8. Bulletin of Earthquake Engineering . 2016;14(3):747–67. https://doi.org/10.1007/s10518-015-9846-7
[21] Berto L, Bovo M, Rocca I, Saetta A, Savoia M. Seismic safety of valuable non-structural elements in RC buildings: Floor Response Spectrum approaches. Eng Struct. 2020; 205:110081.
[22] Shang Q, Li J, Wang T. Floor acceleration response spectra of elastic reinforced concrete frames. Journal of Building Engineering. 2022; 45:103558.
[23] Landge M V, Ingle RK. Comparative study of floor response spectra for regular and irregular buildings subjected to earthquake. Asian Journal of Civil Engineering. 2021; 22:49–58.
[24] Singh MP, Suárez LE. Seismic response analysis of structure–equipment systems with non-classical damping effects. Earthq Eng Struct Dyn. 1987;15(7):871–88.
[25] Perez YM, Guerra EM, Bazan-Zurita E. Seismic Response Of Equipment Supported On Structures. 2015.
[26] Chanda A, Debbarma R. Probabilistic seismic analysis of base isolated buildings considering near and far field earthquake ground motions. Structure and Infrastructure Engineering. 2021;18(1):97–108.
[27] Davoodi M, Sadjadi M, Goljahani P, Kamalian M. Effects of near-field and far-field earthquakes on seismic response of sdof system considering soil structure interaction. In: 15th World Conference on Earthquake Engineering Lisbon, Portugal. 2012.
[28] Alhan C, Öncü-Davas S. Performance limits of seismically isolated buildings under near-field earthquakes. Eng Struct. 2016;116:83–94.
[29] Moghaddam PK, Manafpour AR. Effects of Far-and Near-Field Multiple Earthquakes on the RC Single Degree of Freedom Fragility Curves Using Different First Shock Scaling Methods. International Journal Of Engineering. 2018;31(9):1505–13.
[30] Faghihmaleki H, Ahmadian F, Roosta H. The effect of far field and near field earthquakes on the hysteresis energy and relative displacement of steel moment resisting frame structures. Journal of Building Pathology and Rehabilitation. 2017; 2:1–9.
[31] Tavakoli HR, Naghavi F, Goltabar AR. Dynamic responses of the base-fixed and isolated building frames under far-and near-fault earthquakes. Arab J Sci Eng. 2014; 39:2573–85.
[32] BIS Bureau of Indian Standards. IS 875-2 (1987): Code of Practice for Design Loads (Other Than Earthquake) For Buildings And Structures, Part 2: Imposed Loads.
[33] 2016 IS 13920: Ductile design and detailing of reinforced concrete structure subjected to seismic force. Bureau of Indian Standard (BIS). 2016;
[34] SeismoStruct S. Release-1-A Computer Program for Static and Dynamic Nonlinear Analysis of Framed Structures. 2016.
[35] Engineers AS of C. Seismic evaluation and retrofit of existing buildings. In American Society of Civil Engineers; 2017.
[36] Reinforced Concrete Buildings with Restricted Ductility. In: Seismic Design of Reinforced Concrete and Masonry Buildings . John Wiley & Sons, Ltd; 1992. p. 639–61. https://onlinelibrary.wiley.com/doi/abs/10.1002/9780470172841.ch8
[37] A. Minimum Design Loads and Associated Criteria for Buildings and Other Structures. 2016.
[38] ATC. Quantification of building seismic performance factors. Fema P695. 2009;(June):421.
[39] IS 875 (part 1). IS 875-1: Code of Practice For Design Loads (Other Than Earthquake) For Buildings And Structures, Part 1: Dead Loads. Bureau of Indian Standards, New Delhi. 1987;875(July):1–37.

[40] Shooshtari M, Saatcioglu M, Naumoski N, Foo S. Floor response spectra for seismic design of operational and functional components of concrete buildings in Canada. Canadian Journal of Civil Engineering. 2010 Oct 22; 37:1590–9.

[41] Washington DC. NEHRP (National Earthquake Hazards Reduction Program) Recommended Seismic Provisions for New Buildings and Other Structures (FEMA P-750) Prepared for the Federal Emergency Management Agency of the U.S. Department of Homeland Security By the Building Seismic Safety Council of the National Institute of Building Sciences Building Seismic Safety Council A council of the National Institute of Building Sciences . 2009. www.bssconline.org

[42] British Standards Institution., European Committee for Standardization., British Standards Institution. Standards Policy and Strategy Committee. Eurocode 8, design of structures for earthquake resistance. British Standards Institution; 2005.